

Inverse Synthetic Aperture Imaging using a 40 kHz Ultrasonic Laboratory Sonar

A. J. Wilkinson, P. K. Mukhopadhyay, N. Lewitton and M. R. Inggs

Radar Remote Sensing Group
Department of Electrical Engineering
University of Cape Town, South Africa

ajw@eng.uct.ac.za pradip@rrsg.ee.uct.ac.za

Abstract

A sonar system operating at 40 kHz in air has been developed to allow the capture of acoustic data in a laboratory environment. The system can serve as a teaching tool for students in seismology, sonar and radar, as well as a useful tool for the development and testing of signal and image processing algorithms. The system can be used for monostatic or bistatic modes of imaging. Range compression is achieved by deconvolution filtering which compensates for the linear system effects of the transducers and other components. A deconvolution filter is generated via a calibration technique in which the system response is measured by pointing the transmitting transducer directly at the receiving transducer. Results are presented which demonstrate the capability of the system for range profiling and 2-D imaging, using the inverse synthetic aperture technique whereby the scene to be imaged is moved across the beam of the sensor. The focused image is obtained by synthetic aperture azimuth focusing / migration techniques. The range and azimuth resolutions achieved with system are discussed.

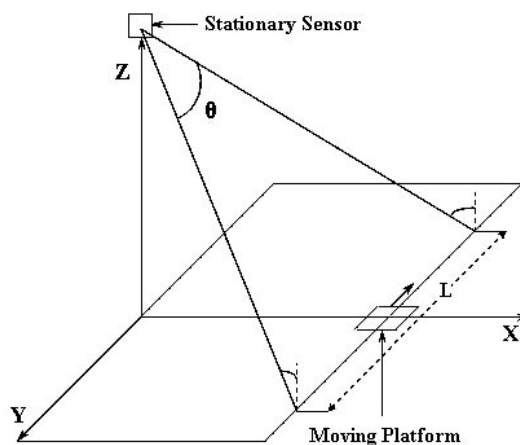
1. Introduction

Obtaining seismic or radar data in real geophysical applications is a time-consuming and expensive process. For those working in this field, the availability of a smaller scale laboratory measurement system operating in air or water [1] is of potential benefit as it allows easy experimentation with different imaging geometries.

A sonar system operating in air at 40 kHz has therefore been developed as a means of acquiring acoustic data in the laboratory environment. The system has proved useful both as a teaching tool for students learning about signal processing techniques employed in seismology, sonar and radar, as well as a tool for developing and testing new signal processing algorithms.

Traditional seismic imaging usually involves gathering data acquired from a multitude of sensors, which together form a large discretely sampled receiving aperture. A high resolution image is obtained by *migration* processing [2, 3].

In the related fields of radar and sonar, the technique known as *synthetic aperture radar/sonar* (SAR or SAS), [4], involves the formation of an aperture by moving a single sensor past a scene of interest along a track. Alternatively an aperture may also be synthesized by keeping the sensor stationary, and relying on the movement of the object of interest past the sensor [5], as depicted in Figure 1 - this approach is known as inverse synthetic aperture imaging (ISAR or ISAS), and is the basis of the imaging technique applied to the 40 kHz sonar described in this paper.



L is the Synthetic Aperture length and θ is the azimuth beamwidth.

Figure 1: Inverse Synthetic Aperture imaging geometry.

The paper is structured as follows: firstly the system hardware and ISAS imaging geometry are briefly described; thereafter the signal processing and calibration techniques developed to focus the images are described; lastly results from an ISAS experiment are discussed.

2. System Hardware

The philosophy behind the sonar hardware was to design a system based around a PC sound, which could be easily operated from within the MATLAB programming environment, and which would also demonstrate hardware techniques, such as frequency heterodyning, employed in radar systems. The initial prototype was developed as an undergraduate student project at the University of Cape Town [6].

A centre frequency of 40 kHz was chosen for the transmitted pulse, which travels at approximately 340 m/s in air; the corresponding wavelength of 8.5 mm is a practical dimension for the scale of imaging. Piezoelectric transducers were readily available with bandwidths of 4 kHz, corresponding to an achievable range resolution of about 4 cm.

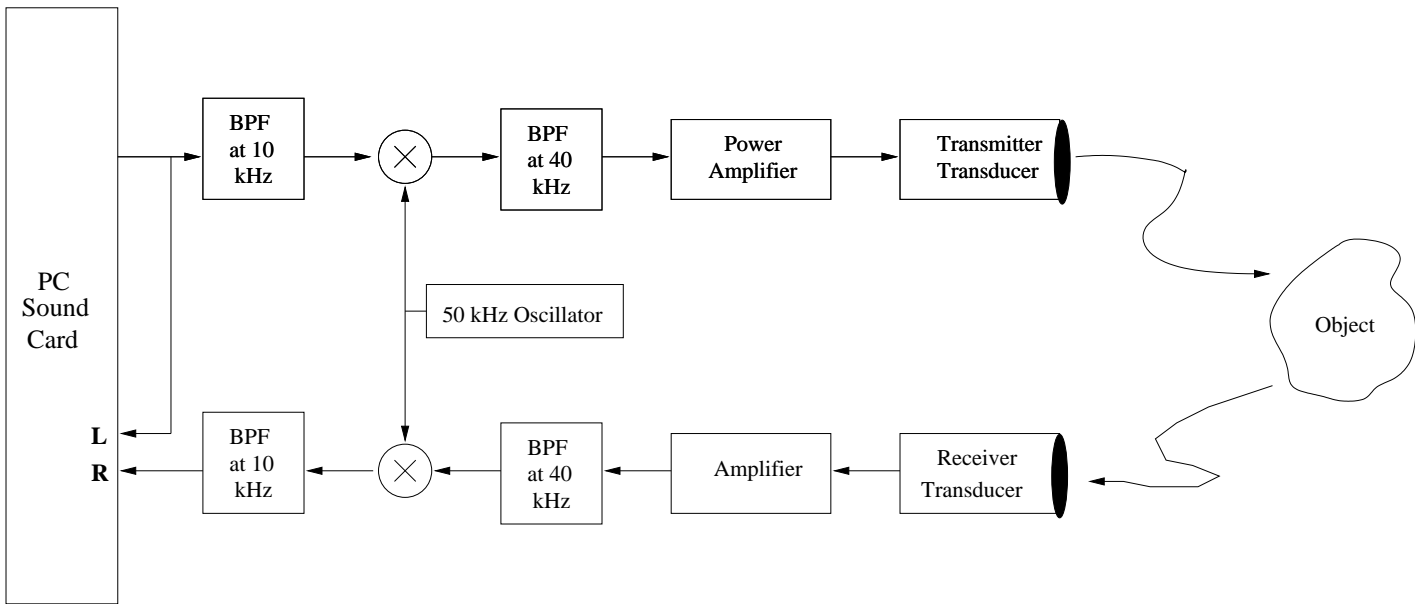


Figure 2: Sonar hardware block diagram.

2.1. Receiver-Transmitter Hardware

A block diagram of the system hardware is shown in Figure 2. MATLAB is used to control the PC sound card, which generates a chirp pulse with spectral components in the audio range between 8 kHz and 12 kHz. This pulse is then mixed with a 50 kHz oscillator, generating a lower sideband at 40 kHz and an upper sideband at 60 kHz. The 40 kHz sideband is passed through a bandpass filter, amplified and fed to the transmitter transducer.

The pulse radiates, is reflected from the scene, and the echo is received by a receiving transducer. The transducers are as shown in Figure 3. The two-way 3 dB beamwidth is approximately 40 degrees. The received signal is amplified and translated down again into the audio range of the sound card, sampled and stored for subsequent digital signal processing. The MATLAB “wavplay” and “wavrecord” commands are used to generate and record the waveforms. The sample rate is set to 44.1 kHz, the maximum rate available on most PC sound cards. In MATLAB, it was not possible to ensure accurate synchronization between the start of playing and recording. This problem was circumvented by simultaneously recording both the transmitted and the received echo on the left and right channels of the sound card as shown in Figure 2, and correlating these recordings.



Figure 3: Piezoelectric 40 kHz transmitter and receiver transducers.

2.2. Moving Platform

To implement the inverse synthetic aperture technique, the scene must be moved across the beam as illustrated in Figure 1. A wooden platform on wheels (Figure 4) was constructed with dimensions 2.5x1.0 m. The platform can be pulled manually by means of a cord, and its position along its track recorded by an accurate odometer wheel [7], which can be seen on the left hand side of Figure 4. The transmitter is synchronized to the odometer, such that pulses are transmitted and recorded at regular spatial intervals along the track.

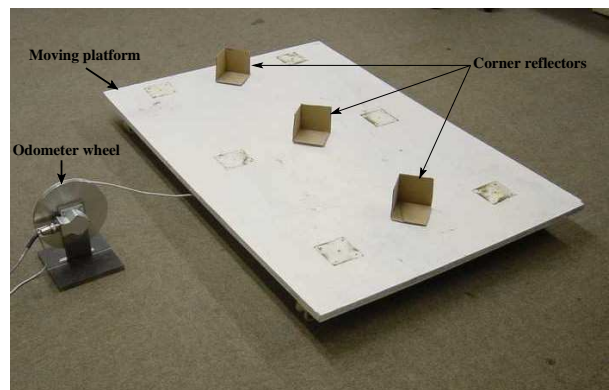


Figure 4: Moving platform containing three corner reflectors.

3. Signal Processing Techniques

The focused image is formed using correlation-type processing, carried out in two steps:

1. range compression using either matched filtering (for optimal signal to noise ratio) or deconvolution processing with frequency domain windowing (for optimal point target response).
2. azimuth focusing using standard migration processing (also known as synthetic aperture focusing), which again may be tailored to give either optimal SNR or optimal point target response.

The results of matched filtering theory under white noise conditions show that the signal to noise ratio is proportional to the energy in the received signal, whereas the resolution is a function of the signal bandwidth [4].

The transmitted pulse was chosen to be a chirp pulse, commonly used in radar applications to satisfy the simultaneous requirements of high energy and wide bandwidth. In the chirp waveform, the instantaneous frequency of a sine wave is swept linearly over time, modelled by,

$$v_{tx}(t) = \text{rect}\left(\frac{t}{T}\right) \cdot \cos(2\pi[f_0 t + 0.5Kt^2])$$

where f_0 is the centre frequency, T is the pulse length and $K = \frac{B}{T}$ is chirp rate in Hz/sec. A pulse length of $T = 8$ ms was used corresponding to a physical extent in air of 2.7 m.

The recorded complex baseband signal may be modelled by

$$V_{bb}(f) = H_s(f)\zeta(f + f_0) + N(f + f_0)H_{rec}(f)$$

where $\zeta(f + f_0)$ is a basebanded version of the analytic representation of the impulse response of the target scene, and $N(f + f_0)$ is the basebanded noise referred to the input of the first amplifier. All linear system effects affecting the target response are modelled by the equivalent baseband system transfer function

$$H_s(f) = P(f)H_1(f)H_2(f)H_3(f)H_4(f)H_5(f)H_6(f)$$

where H_1 models the first BPF at 10 kHz, H_2 the BPF and power amplifier at 40 kHz, H_3 the transmitting transducer, H_4 the receiving transducer, H_5 the receiver amplifier and BPF at 40 kHz, and H_6 the BPF at 10 kHz. The function $P(f)$ models the baseband transmitted pulse. The noise is shaped by receiver transfer function $H_{rec}(f) = H_5(f)H_6(f)$.

3.1. Range Profiling

The pulse bandwidth was chosen to be 4 kHz, covering the passband of the transducers. For optimal SNR, under additive noise conditions, the received echo is processed by matched filtering, i.e. the output signal is computed by

$$v_0(t) = \mathcal{F}^{-1}[H_{MF}(f) \cdot V_{bb}(f)]$$

for which $H_{MF}(f) = H_s^*(f)/\sqrt{S_n(f)}$ where $S_n(f)$ is the power spectral density of the noise. If passband is fairly flat, with white noise, then $H_{MF}(f) \approx P^*(f)$.

Although optimal for SNR, matched filtering results in an undesirable point target response if the passband of the transducers are not flat in magnitude and linear in phase. This is

the case in this sonar system, as the desired 4 kHz bandwidth extends into the roll-off of the transducers.

Instead, a deconvolution processing approach was adopted, in which the baseband signal is passed through the filter $H(f) = [1/H_s(f)]\text{rect}(f/B)$. A special calibration procedure was developed in which the transmitter transducer was aimed directly at the receiving transducer, separated by a distance d equal to two metres. This allowed direct recording of the total system response, allowing $H_s(f)$ to be obtained.

With this filter, the processed baseband response is given by

$$V(f) = \text{rect}(f/B)\zeta(f + f_0)$$

For a point target at range r modelled by $\zeta(t) = \zeta_0\delta(t - \tau)$ where ζ_0 is the reflection coefficient, and $\tau = 2r/c$, the processed frequency response is

$$V(f) = \text{rect}(f/B)\zeta_0 e^{-j2\pi(f+f_0)\tau}$$

with a corresponding $Sa()$ shaped time response

$$v(t) = \zeta_0 B S a(\pi B(t - \tau)) \cdot e^{-j2\pi f_0 \tau}$$

The corresponding 3dB range resolution, is $\delta R \approx \frac{0.89c}{2B} = 3.8$ cm. Frequency domain windowing may also be applied to reduce the sidelobe levels in the response. Application of a Hamming window reduces the first sidelobe to 41 dB below the peak, at the expense of main lobe broadening by a factor of 1.5.

3.1.1. Range Compression Processing Steps

Because of the lack of precise synchronization between transmitting the chirp and the start of recording, an additional step is required in which the range profiles time aligned by correlating the recorded echo with the recording of the transmitted waveform. The sequence of steps used to form a range profile are listed below.

- Step 1 The chirp emitted from the output of the sound card and the received echo, are recorded on the left and right input channels and stored in vectors v_{tx} and v_{rx} . These signals lie in the 8-12 kHz intermediate frequency band, centred on frequency $f_{IF} = 10$ kHz.
- Step 2 The received signal v_{rx} is correlated with v_{tx} , in the frequency domain, i.e. $V = FFT(V_{rx}) \cdot FFT(V_{tx})^*$.
- Step 3 The deconvolution filter is applied (its formation is described below).
- Step 4 A Hamming window is applied.
- Step 5 The signal is converted to a complex analytic signal, by zeroing out the negative frequency components, and inverse transforming to the time domain.
- Step 6 The complex baseband signal is formed by multiplying by $e^{-j2\pi f_{IF} t}$. This operation translates the spectral components down to baseband.

The creation of the deconvolution filter involves the following steps:

- The transducers are pointed towards one another with a separation distance of $d = 2$ m.
- Steps 1 and 2 above are carried out to obtain a time aligned recording.

- To reduce noise, several echoes are averaged and stored in vector v_{ave} , but this must take place after step 2 has been applied, as averaging requires the data to be time aligned.
- A deconvolution filter is created, i.e. $H_d = [1/H_s]e^{-j2\pi ft_d}$ where $H_s = FFT(v_{ave})$ and $t_d = d/c$. A linear phase correction is included to compensate for the 2m separation of the transducers. This will ensure that application of the deconvolution filter to a received echo does not result in a 2m range shift.

3.2. Azimuth Focusing

Azimuth focusing was achieved using standard *time domain synthetic aperture processing* [4], which is computationally inefficient, but accurate for non-linear trajectories. A point in the focused image is constructed by coherently adding the data collected along the hyperbolic contour in the range compressed data matrix. In complex baseband form, this requires phase correcting each data point prior to addition. The azimuth resolution is a function of the azimuth spatial bandwidth i.e. $\delta x \approx \frac{1}{B_x}$, where $B_x \approx \frac{4 \sin(\theta/2)}{\lambda_0}$ is the bandwidth in cycles per metre, θ is the azimuth beamwidth to be processed in radians, and λ_0 is the wavelength. For a two-way idealized beamwidth of approximately 40 degrees, the spatial bandwidth is approximately 162 cycles/metre, and the expected azimuth resolution is approximately 6 mm.

As with the range response, the sidelobe levels of the resulting azimuth point target response may be tailored by appropriately weighting of the summed echoes.

4. Experimental Results

To demonstrate the potential for inverse synthetic aperture imaging, a target scene (photograph in Figure 4) consisting of three corner reflectors constructed from stiff cardboard, was dragged across the beam as illustrated in Figure 1. Pulses were transmitted at 5 mm intervals as the scene progressed along the track, satisfying the azimuth Nyquist criterion $\Delta x < \frac{1}{B_x}$. Additionally, every 10 cm, the corner reflectors were carefully manually rotated about their phase centres to point in the direction of the transducers, hence simulating the angle independent response of ideal point targets.

A plot of a single downrange profile showing the three targets after range compression using a deconvolution filter with Hamming window, and compensation for R^2 loss is shown in Figure 5. The 3 dB range resolution was measured to be 5.83 cm, close to the expected value of 5.55 cm. A comparison between the deconvolution and matched filter responses is shown in Figure 6. In both cases a Hamming window was applied. The pulse compression of deconvolution filter response is improved compared to the match filtered response.

The range compressed profiles were assembled into a matrix, displayed in Figure 7. The point targets result in characteristic hyperbolic shaped signatures.

These data were then compressed in azimuth, and the resulting image is shown in Figure 8. Figure 9 shows a cross section, cutting through the 2nd target in the azimuth direction. The same cross section is shown on a dB scale in Figure 10. The 3dB width of the azimuth compressed main lobe was measured to be 0.82 cm, slightly greater than 0.55 cm value calculated with the approximate 40 degree beamwidth. The difference is attributed to lack of accurate compensation for the amplitude

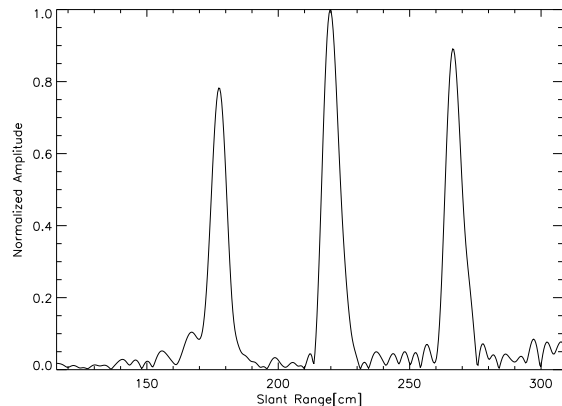


Figure 5: Plot of range compressed profile intersecting three corner reflector targets.

and phase response of the transducer beams, and deviations in the target trajectory from a straight line.

One factor affecting performance of the system was a pulse to pulse fluctuating phase shift in the observed point target response which was the result of variations in the propagation medium. It was observed that even light air disturbances, would result in phase shifts of as much up 20% of a wavelength. A still air environment does however have sufficient phase stability for coherent imaging.

	Expected [cm]	Measured [cm]
Range Resolution	5.55	5.83
Azimuth Resolution	0.55	0.82

Table 1: 3-dB resolutions in range and azimuth.

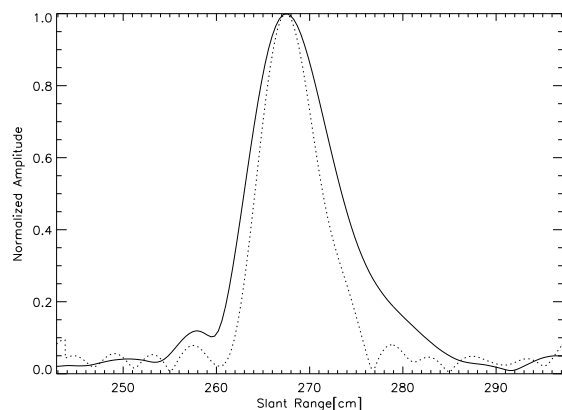


Figure 6: Comparison between matched filter and deconvolution filter responses - in both cases a Hamming window was also applied.

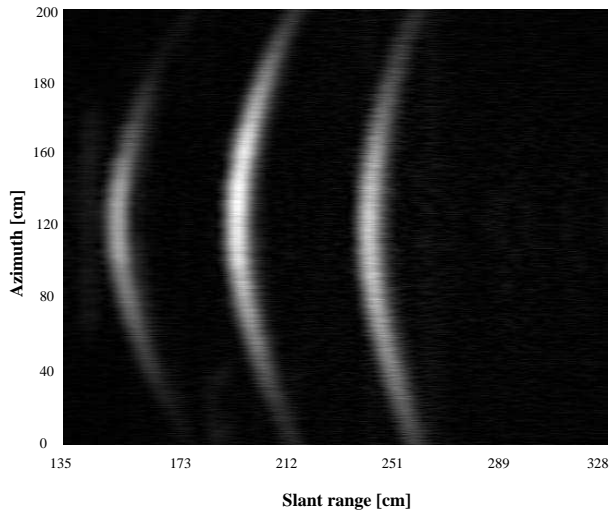


Figure 7: Range compressed data matrix, prior to azimuth compression.

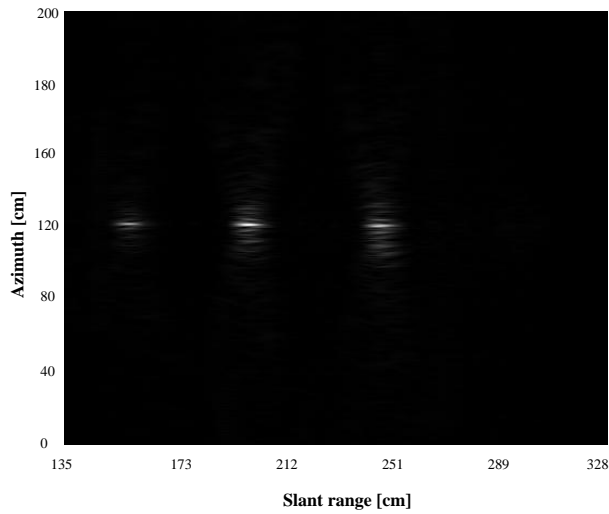


Figure 8: Image after azimuth compression.

5. Conclusions

This work has demonstrated the use of a 40 kHz air-based sonar for conducting coherent imaging experiments in a laboratory scale environment. The results show the application in range profiling and 2-D inverse synthetic aperture imaging. The system has proved to be an excellent tool for teaching and experimenting with radar and sonar concepts.

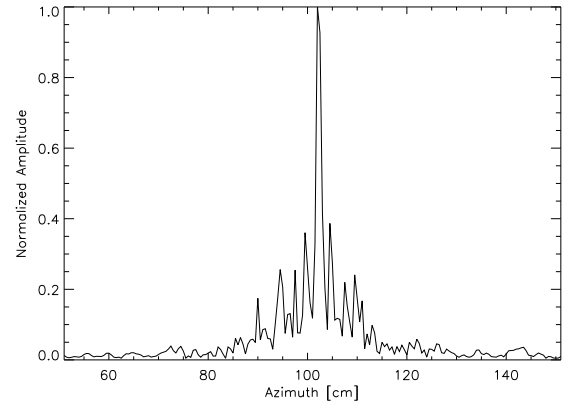


Figure 9: Cross section of a single target in azimuth direction.

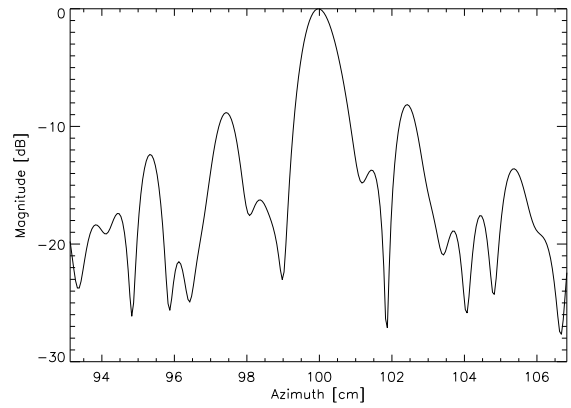


Figure 10: dB plot of the azimuth cross section.

6. References

- [1] Mason, I. Osman, N. Liu, Q. Simmat, C. and Li, M., "Broadband Synthetic Aperture Borehole Radar Interferometry", *Journal of Applied Geophysics*, Vol. 47,299–308, 2001.
- [2] Yilmaz, Ö., "Seismic Data Analysis, Society of Exploration Geophysicists", Vol. I, 2001.
- [3] Berkhout, A. J., "Wave field extrapolation techniques in seismic migration, a tutorial", *Geophysics*, Vol. 46(12),1638–1656, 1981.
- [4] Bamler, R. and Schattler, B., "SAR Data Acquisition and Image Formation, Ch. 3 in book *Geocoding: ERS-1 SAR Data and Systems*",1993.
- [5] Wehner D. R., "High Resolution Radar", Ch. 7, Artech House, 1987.
- [6] Korda, S. and Trinic, M., "Design and Construction of an Ultrasonic Radar Emulator", BSc Thesis, Department of Electrical Engineering, University of Cape Town, 2002.
- [7] Nyareli, T., "Development of a Cable Odometer with a Network Interface", MSc Thesis, Department of Electrical Engineering, University of Cape, 2003.